

TSW-YOLO-v8n: Optimization of Detection Algorithms for Surface Defects on Sawn Timber

Mingtao Wang,^a Mingxi Li,^b Wenyan Cui,^a Xiaoyang Xiang,^a and Huaqiong Duo^{a,*}

The goal of this work was to better meet the demand for rapid detection of surface defects in sawn timber in forestry production. This paper introduces a two-way feature fusion network based on the YOLO-v8 algorithm and proposes a feature fusion network model that combines the attention mechanism and loss function optimization. In this way it increases the tiny target detection head in order to more effectively detect small defective targets in the wood, thus realizing the model's high-efficiency and low-consumption functional design. The results show that the improved TSW-YOLO-v8n model realized the identification of eight kinds of defects in sawn timber with a high efficiency of 91.10% mAP50 and an average detection 6 ms, which is 5.1% higher than the original model's mAP50 and 1 ms shorter than the original model's average detection time. The comparison of the original model and its mainstream algorithms shows that the model of this paper had better performance and better detection capability. Thus, the improved model achieved better overall performance and stronger detection ability, which provides a new idea for the development of detection technology in the forestry industry.

DOI: 10.15376/biores.18.4.8444-8457

Keywords: Deep learning; Target detection; Surface defects of sawn timber; YOLO-v8; Attention mechanism; Loss function; Feature fusion

Contact information: a: College of Materials Science and Art Design, Inner Mongolia Agricultural University, Hohhot 010018, P.R. China; b: Zhengzhou Research Base, State Key Laboratory of Cotton Biology, School of Agricultural Sciences, Zhengzhou University, Zhengzhou 450001, Henan, China;

* Corresponding author: duohuaqiong@163.com

INTRODUCTION

In the era of artificial intelligence, the wood industry is undergoing a profound transformation as it embraces a multitude of cutting-edge technologies, striving to integrate with emerging industries and achieve a high level of automation and intelligence. One particularly active area of technological exploration is the application of deep learning techniques to detect surface defects in wood.

Traditional manual inspection methods for wood surface defects are marred by their inherent inefficiencies. They are time-consuming, demand a substantial labor force, and are generally inefficient (Qayyum *et al.* 2016). However, machine-based wood defect detection methods, although effective, bring their own set of challenges, including safety hazards, high costs, and intricate operational procedures.

In stark contrast, the convergence of computer-based image processing techniques and deep learning technology, operating at the nanoscale level and harnessed by high-performance processing units such as GPUs, presents a compelling solution. This approach boasts many advantages, including rapid processing speeds, cost-effectiveness, and ease of operation. These qualities make it exceptionally adept at identifying and classifying faults

in wood. This fusion of technologies offers a promising pathway to revolutionizing wood defect detection with efficiency and precision (Yang *et al.* 2018).

Intelligent detection of wood defects can be categorized into two types, based on different prediction methods and processing procedures. The first type is single-stage wood defect detection, which is also known as a target detection algorithm based on regression analysis. This algorithm only requires one feature extraction to perform regression analysis on the target location and category information. The detection results are then output using a neural network model (Zhu *et al.* 2023). Common single-stage algorithms include OverFeat, the YOLO series, SSD, and RetinaNet. The second type is two-stage wood defect detection, also known as the target detection algorithm, based on region suggestions. This algorithm converts the target detection problem into processed suggested region image classification through explicit region suggestions. Common two-stage algorithms include R-CNN, SPP-Net, Fast R-CNN, and Faster R-CNN. These two algorithms have their respective advantages and disadvantages. Single-stage algorithms perform classification and regression directly without generating candidate regions, thus ensuring high efficiency and suitability for real-time object detection. However, they suffer from lower accuracy in detecting clustered objects and small targets. Two-stage algorithms, on the other hand, first generate candidate regions and then perform classification and regression. The benefit of this approach is higher algorithm accuracy, making it suitable for precision-driven object detection. However, this comes at the cost of reduced real-time detection capabilities and less effective small object detection.

YOLO-v1 (the first version of You Only Look Once) network, the pioneer of YOLO series, was produced in 2016. It has received widespread attention due to its mechanism of direct target localisation and stereotyping of the target to be inspected without the need for pre-extraction of candidate features, which reduces the resource consumption and also improves the speed of the inspection. Wang *et al.* (2021a) proposed separable convolutional ideas to improve the YOLO-v3 network, but only in the recognition of the accuracy and speed of the improvement, for small defects such as cracks and small holes in the recognition of low efficiency. Kurdthongmee (2023) built a framework for a wood defect detection system based on YOLO-v3, which focuses on training the dataset so that it can meet the requirements of deep learning models in terms of size and variability. However, the method has limitations and the final recognition results are average. Cui *et al.* (2023) proposed an improved method based on the YOLO-v3 network framework with Spatial Pyramid Pool (SSP) network. They obtained an accuracy of 93.23% for identification of wood defects in a test set with an industrial production detection time of less than 13 ms. Wang *et al.* (2021b) proposed an improved version of YOLO-v4 network and successfully achieved the identification and classification of live knots, dead knots, cracks, and insect eyes on the surface of domestic spruce sawn timber. However, YOLO-v4, as an enhanced version of YOLO-v3, has not changed its core idea, and still has the problem of misclassification and omission of small defects such as fine cracks and small holes.

Based on the fact that the YOLO series does not make outstanding improvements for small defects on the surface of wood, Fang *et al.* (2021) focused on the detection and identification of wood knots. They used the YOLO-v5 detector to adaptively learn and extract knots on the surface of sawn timber. Unfortunately, they used the YOLO model for detecting knot defects and did not conduct experiments on knot classification, so the usefulness of the YOLO-v5 network for classifying wood knots has yet to be demonstrated. Cao *et al.* (2023) proposed a YOLOv5-LW method for detecting defects in lightweight wood boards. Their system combines the attention mechanism and feature fusion network

to solve the problems of slow detection speed and difficulty in deploying embedded devices for defect detection in wood boards. The approach reduces the number of parameters and computation of the whole model and improves the detection speed while improving the recognition accuracy. At present, the existing research on wood defect detection mainly has focused on detecting a single type or a few common defects, which cannot meet the needs of more delicate wood processing. Han *et al.* (2023) optimised the backbone network while introducing BiFPN in the neck to achieve a multi-scale weighted bidirectional feature fusion STC-YOLOv5, which achieved a better detection effect for the seven types of defects and has great potential for application in the field of forestry industry.

The YOLO series of algorithms is well-regarded for their efficient detection capabilities, modular design, and simplicity, making them an attractive choice for single-stage target detection tasks. Over time, various optimized and enhanced models within the YOLO series have emerged, gaining application in diverse fields, including wood defect detection. These algorithms, both in their basic form and as improved models, have significantly propelled the advancement of defect detection technology within the timber industry. They represent a valuable technological asset for improving production and enhancing the quality of life.

Addressing the specific requirements of the wood industry, particularly the challenge of detecting small defects, this paper introduces an improved YOLO-v8 algorithm, denoted as TSW-YOLO-v8n. The primary objective of this enhanced algorithm is to excel in the detection of small defects while keeping computational resource requirements manageable. It strives to enhance the accuracy and speed of detecting surface defects in sawn timber, meeting the demand for high-precision real-time detection.

The proposed algorithm's performance is rigorously validated using a custom-made dataset, ensuring that it meets the stringent requirements for defect detection tasks within the wood industry. This research contributes to advancing the state-of-the-art in wood defect detection and reflects the ongoing evolution of YOLO-based algorithms for diverse applications. The main contributions of this study are:

1. Adding tiny target detection heads to improve the ability of the YOLO-v8 model for small defect detection.
2. Fusing YOLO-v8 model using the Triplet Attention mechanism to further improve the model's ability to detect small defects.
3. Adopting BiFPN bidirectional cross-scale connectivity with weighted feature fusion to improve the accuracy and efficiency trade-off of the model.
4. Introducing the Wise-IoU loss function to enhance the ability of YOLO-v8 model to capture information and improve the defect information learning ability.

EXPERIMENTAL

Wood Defects Dataset

The dataset used for the experiment was from a large dataset of wood surface defect images provided by (Kodytek *et al.* 2022). To ensure the reliability and utility of the experimental data, a screening process was conducted based on the original dataset. This screening resulted in the selection of 3,612 defective wood defect images (as shown in Fig. 1). To augment the dataset and enhance its diversity, various image processing techniques were applied. Specifically, six methods were employed, including random combinations

of pixel point removal, sharpening, affine transformation, brightness adjustment, random hue modification, and horizontal flipping. These methods were randomly applied to the original defective images, generating a total of 18,060 augmented defective datasets. When combined with the original images, this resulted in a dataset comprising 21,672 images in total.

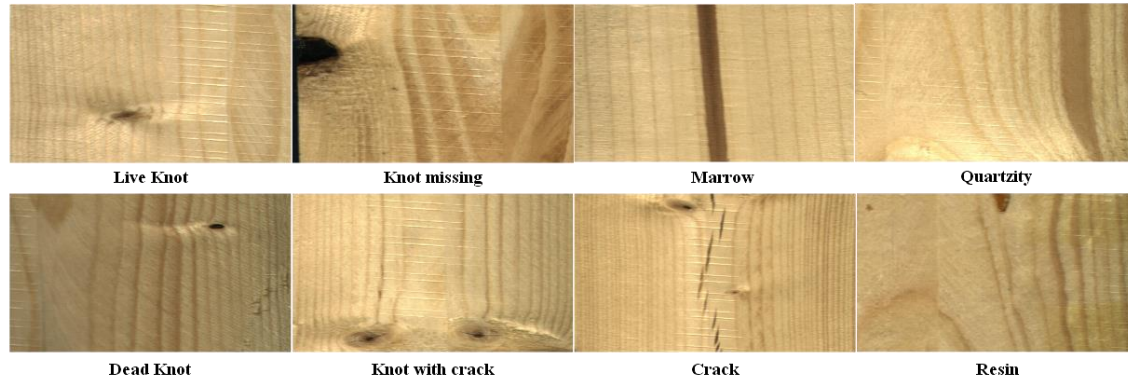


Fig. 1. Eight kinds of defects on the surface of sawn timber

To facilitate the machine learning experiments, the dataset was divided into three subsets: a training set, a validation set, and a test set, distributed in an 8:1:1 ratio. This division ensures that the dataset is appropriately utilized for model training, validation, and evaluation, respectively.

The enhanced dataset utilized in this study encompasses eight distinct types of defects, including live knots, dead knots, and cracks, among others. Figure 2 provides relevant insights into the characteristics of these defects within the dataset:

1. Figure 2-a presents an overview of the distribution of various defects in the dataset. It is notable that live and dead knots predominate in the dataset, mirroring real-world scenarios.
2. Figure 2-b illustrates the size distribution of the bounding boxes for different defects in the dataset.
3. Figure 2-c offers an insight into the distribution of coordinates for the center points of the bounding boxes for various defects. It appears that the center points are concentrated towards the middle of the bounding boxes.
4. Figure 2-d displays a scatter plot showing the relationship between the width and height of the defective bounding boxes. The concentration of dark-colored blocks in the lower-left corner indicates that small defects constitute the majority of instances in this dataset.

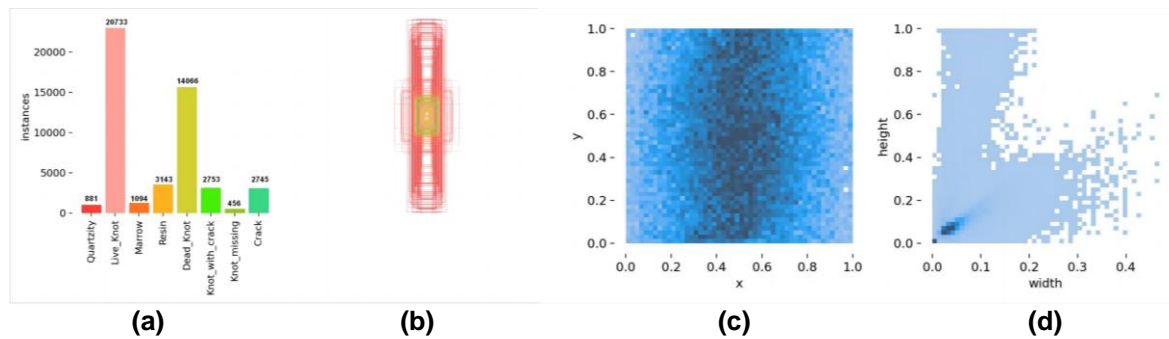


Fig. 2. Dataset infographic

These visualizations provide valuable information about the composition and characteristics of the dataset, highlighting the prevalence of certain defect types and their size distribution.

TSW-YOLO-v8n

The YOLO-v8 model represents a significant advancement in object detection and instance segmentation, building upon the foundations of the previously introduced YOLO-v5 by ultralytics at the beginning of 2023. YOLO-v8 not only achieves enhanced speed and accuracy compared to its predecessors but also extends its capabilities to support a range of tasks, including image classification, object detection, and instance segmentation. This makes it a versatile and high-performance algorithmic model suitable for multitasking scenarios.

For this paper's objectives, YOLO-v8n was chosen as the base model for enhancement, considering practical real-world considerations. YOLO-v8n was selected because it offers a relatively small pre-training model size of only 6MB, making it suitable for deployment on mobile devices, while also maintaining a fast detection speed.

However, YOLO-v8n's detection performance, although fast, does not meet the rigorous requirements of factory applications when it comes to detecting surface defects on sawn timber. To address this, this paper introduces four key improvements to YOLOv8, resulting in the development of an advanced intelligent detection model called TSW-YOLO-v8n. These enhancements encompass the addition of a tiny target detection head, the incorporation of an attention mechanism, the integration of a feature fusion mechanism, and the optimization of the loss function. The schematic structure of the improved TSW-YOLO-v8n model is visually depicted in Fig. 3, showcasing the novel architecture designed to achieve superior performance in the detection of surface defects in sawn timber.

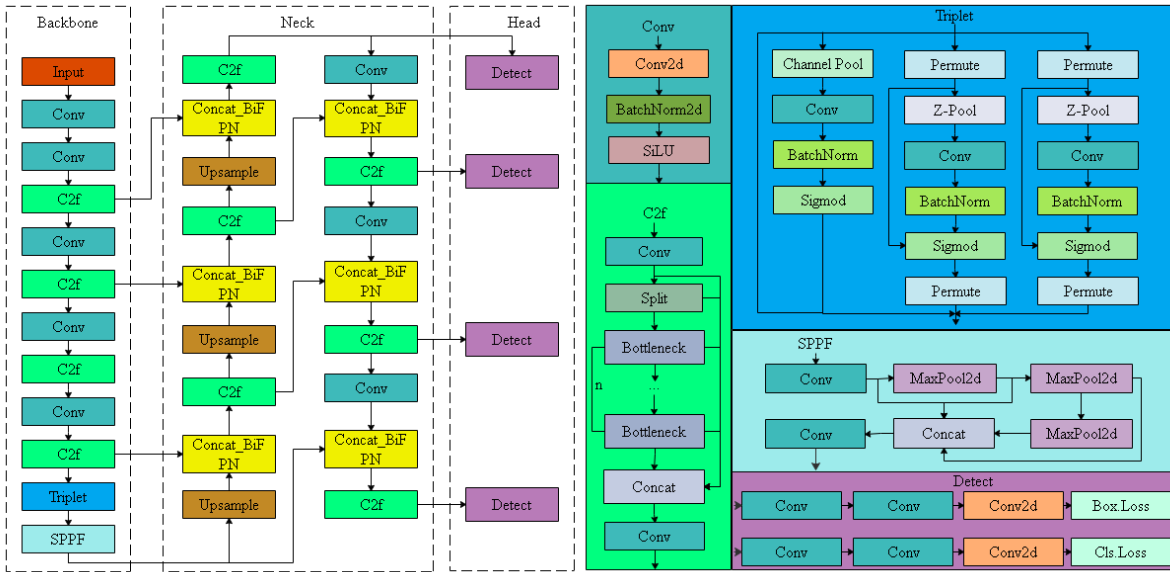


Fig. 3. TSW-YOLO-v8n structure diagram

Small target detection head

To enhance the YOLOv8 model's capability for detecting small targets, a novel small-target detection head was introduced in response to the specific requirements of this paper's dataset. This new detection head is seamlessly integrated with Bi-FPN features, effectively bolstering the model's performance when it comes to detecting small targets.

This strategic addition and fusion of features cater to the unique characteristics of the dataset, ensuring that the model excels in identifying and accurately detecting small targets, further enhancing its overall detection performance.

Triplet Attention mechanism

Wood, as a natural plant material, exhibits a significant challenge in defect detection due to the seamless integration of defects with the wood itself. Sawn timber defects often blend into the background, making them challenging to detect. To address this issue, the Triplet Attention mechanism is introduced to enhance the YOLO-v8 model's ability to capture information interactions across different dimensions. This augmentation aims to improve the model's capacity to detect defects when they are intertwined with the texture background of sawn timber.

Furthermore, the Triplet Attention mechanism is engineered to be computationally efficient while delivering substantial performance improvements. This efficiency aligns with the practical requirements of the enhanced YOLO-v8 model, particularly for the deployment of mobile inspection devices.

In this paper, the Triplet Attention mechanism is integrated after the last C2f module of the YOLO-v8 backbone network. This strategic placement addresses the challenge of defects blending into the background, redirecting the network's attention towards surface defects on sawn timber and effectively separating them from the background during the inspection task. The schematic diagram illustrating this integration is presented in Fig. 4.

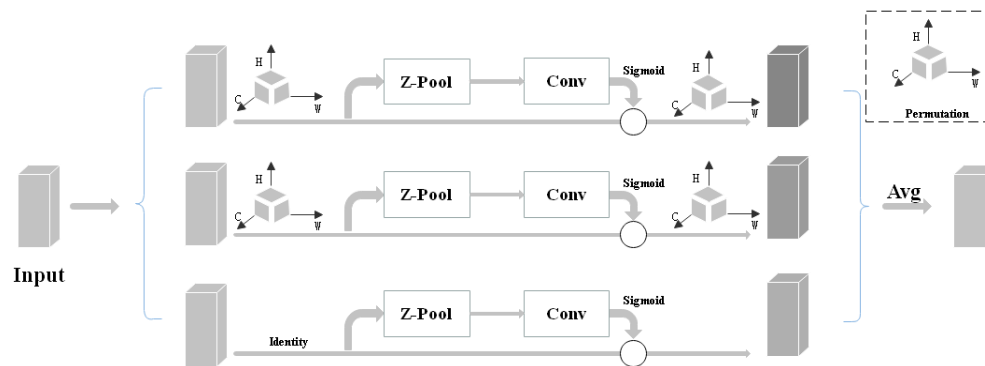


Fig. 4. Triplet Attention structure diagram

The Triplet Attention mechanism (Misra *et al.* 2020) is structured with three parallel branches. Two of these branches are responsible for capturing interactions across different dimensions: one focuses on interactions between the channel dimension (C) and the spatial dimensions (H or W), and the last one is used in the same way as in Woo *et al.* (2018) to build spatial attention. The outputs of all three branches were combined by averaging their respective weights and then aggregated.

This innovative design with cross-latitudinal interaction addresses the conventional computational model's challenge of separating channel attention and spatial attention. Instead, it captures the spatial dimension's interaction with the channel dimension within the same framework. In essence, it simultaneously captures information interactions in three dimensions: (C, H), (C, W), and (H, W), which represent the interactions between channel, height, and width dimensions of the input data, respectively.

BiFPN feature fusion

The YOLO-v8 model utilizes the Feature Pyramid Network (FPN) to integrate multi-scale features from an image through the conventional top-down pathway. This approach results in the generation of different feature maps by downsizing the image, allowing predictions to be made on each of these feature maps. While this strategy aids the model in identifying targets of various sizes, it comes with several drawbacks, including a high demand for computational resources, sluggish inference times, and a lack of suitability for real-time detection tasks. These limitations do not align with the objectives of this paper.

To address these challenges, the paper introduces the BiFPN (Bidirectional Feature Pyramid Network, Tan *et al.* 2020). The BiFPN mechanism incorporates bidirectional cross-scale connectivity and a weighted feature fusion approach. This enhancement not only bolsters the model's feature extraction capabilities but also mitigates the computational resource overhead. Additionally, it accelerates detection speed and optimizes the model's real-time detection capabilities by adjusting the weights and fine-tuning the contribution of each scale to the feature fusion network. This innovation represents a more efficient and effective approach to multi-scale feature integration for improved model performance.

Figure 5 vividly illustrates the BiPFN (Bilateral Pyramid Feature Network) feature fusion mechanism, which represents a significant departure from the traditional unidirectional information flow in FPN (Feature Pyramid Network) as shown in (a). This innovative approach is designed to enhance the model's efficiency by introducing an additional connection when the original input and output nodes are at the same level. This addition enables the fusion of more features with only a minimal increase in computational cost.

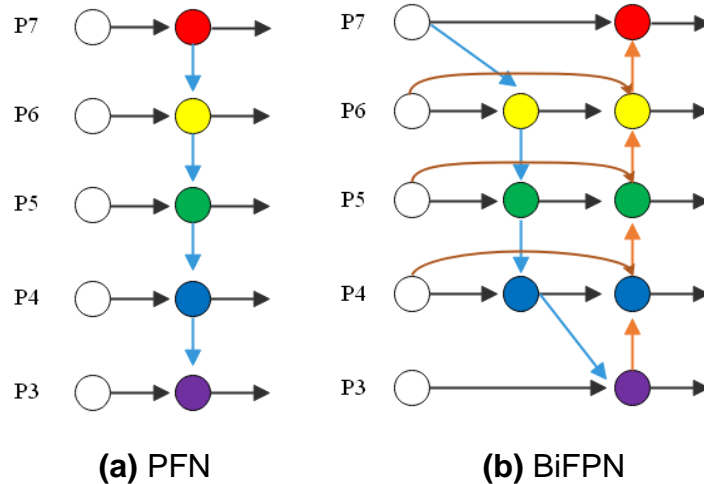


Fig. 5. BiFPN and PFN structure comparison diagram

Moreover, the BiFPN framework incorporates both top-down and bottom-up pathways, which are considered as feature network layers that are recurrently activated. This design choice facilitates extensive feature fusion, significantly amplifying the amount of feature extraction information available to the model. Consequently, this approach augments the model's feature extraction capacity and overall efficiency, effectively meeting the real-time detection requirements.

Wise-Iou loss function

In this study, surface defects in sawn timber, particularly live and dead knots, constitute a significant proportion of the dataset. These defects often present a challenge due to their relatively small sizes. While YOLOv8 employs Distance-IoU (DFL) and Complete-IoU (CIoU) for computing bounding box regression loss, CIoU exhibits limitations. It not only neglects the balance issue between difficult and easy samples but also struggles with accurately representing aspect ratios, resulting in imprecise detection outcomes.

To address these shortcomings, this paper introduces Wise-IoU (Tong *et al.* 2023), a pixel-level semantic segmentation loss function for deep learning models. Wise-IoU is calculated by assessing the similarity between two binary images, essentially quantifying the weighted average of Intersection over Union (IoU) between the predicted segmentation mask and the true segmentation mask. The work by Tong *et al.* presents three versions of Wise-IoU, with version 3 (v3) incorporating attention-based prediction frame loss and the inclusion of focusing coefficients. These enhancements empower the model to better localize defects while leveraging the strengths of EIoU (Enhanced IoU) and SIoU (Scaled IoU), with a particular emphasis on dynamically optimizing loss weights for small defects. This holistic approach contributes to a significant improvement in the detection performance of YOLO-v8.

The specific formula for Wise-IoU v3 is depicted in Eq. 1.

$$L_{WIoUv3} = r L_{WIoUv3}, r = \frac{\beta}{\delta \alpha^{\beta-\delta}} \quad (1)$$

In Eq.1, β denotes outlier, r denotes gradient gain, α and δ are hyperparameters. When $\beta = \delta$, so that $r = 1$, the anchor frame has the highest gradient gain when the outlier of the anchor frame satisfies $= C$ (C is a constant). Therefore it has a dynamic anchor frame quality division criterion, which enables WIoUv3 to give the most appropriate gradient gain allocation strategy at different moments.

Experimental Environment

Experimental environment

The experimental environment configuration is outlined in Table 1. Specifically, the training parameters used in this experiment are as follows:

1. Input image size: 640 pixels
2. Iteration period: 400 iterations
3. Batch size: 16
4. Initial learning rate: 0.001
5. Weight decay coefficient: 0.0005
6. Intersection over Union (IoU) threshold for testing: 0.7

Table 1. Experimental Environment Configuration

Configuration	Version Parameter
System Environment	Windows 10 Professional 21H2
Central Processor	13th Gen Inter(R) Core(TM) i5-13600KF 3.50GHz
Graphics Processor	NVIDIA GeForce RTX 4060Ti 8GB
Graphics Processor Accelerator Library	CUDA 11.8.0, CUDNN8.0
Random Access Storage	32.0 GB
Deep Learning Environment	Pytorch 2.0.1
Deep Learning Frameworks	Python 3.9.16

Performance indicators

In order to assess the detection effect of the improved model, the common evaluation indexes for wood defect detection were selected: Precision, Recall, F₁ Score, mAP and Confusion Matrix.

RESULTS AND DISCUSSION

Comparison with YOLO-v8 and its mainstream models

To substantiate the effectiveness of the enhanced model, TSW-YOLO-v8n, in terms of detection performance, a comparative experiment was conducted against the original YOLO-v8 model. As presented in Table 2, the results underscore the substantial improvements achieved by the enhanced model. Specifically, the mean average precision (mAP) was elevated by 5.1%. Across various defect categories, there were notable enhancements, with the exception of “missing nodes.” Particularly noteworthy is the improved capability to detect small defects, such as live knots, dead knots, and cracks, which exhibit significant performance gains. Furthermore, the improvement in Quartzity detection exceeded 20%. These findings demonstrate that the enhanced model effectively enhanced the detection accuracy of small defects and overall elevated the model’s detection performance.

To further underscore the superiority of the current TSW-YOLO-v8n model, we also comprehensive comparisons and testing were conducted with other prominent models, as detailed in Table 2.

The outcomes of these comparative tests, as presented in the table, unequivocally showcase the exceptional detection performance of the enhanced model proposed within this paper. Notably, while mitigating issues associated with substantial target positioning errors and the challenging task of detecting small targets inherent to the YOLO series, this improved model simultaneously enhanced both recognition and detection capabilities pertaining to small defects.

Table 2. Comparison of Defect Identification Diagrams between YOLO-v8n and Mainstream Models and TSW-YOLO-v8n

Defect Model	Live Knot	Dead Knot	Knot with crack	Knot missing	Crack	Resin	Marrow	Quartzity	mAP
YOLO- v8n	94.7%	94.6%	79.2%	89.6%	92.7%	94.9%	98.0%	44.4%	86.0%
Faster R-CNN (Shih <i>et al.</i> 2019)	77.70%	86.30%	88.30%	88.40%	84.40%	81.80%	85.30%	83.50%	84.80%
SSD (Liu <i>et al.</i> 2016)	61.00%	71.67%	40.27%	66.33%	53.92%	54.66%	59.94%	75.74%	60.44%
YOLO- v5	88.10%	90.90%	71.70%	75.10%	77.80%	90.80%	97.40	50.30%	80.30%
TSW- YOLO- v8n	96.6%	97.7%	88.30%	82.4%	99.0%	97.9%	98.8%	68.5%	91.1%

Figure 6 illustrates the change curves of key evaluation metrics throughout the training process, depicting a comparison between the improved model and the original model. The metrics are presented as follows:

- (a) Comparison of classification loss (cls_loss) between the model's training classification results and actual ground truth annotations.
- (b) Comparison of precision in model recognition.
- (c) Comparison of the mean average precision (mAP) for each individual category.
- (d) Comparison of the recall rate (recall).

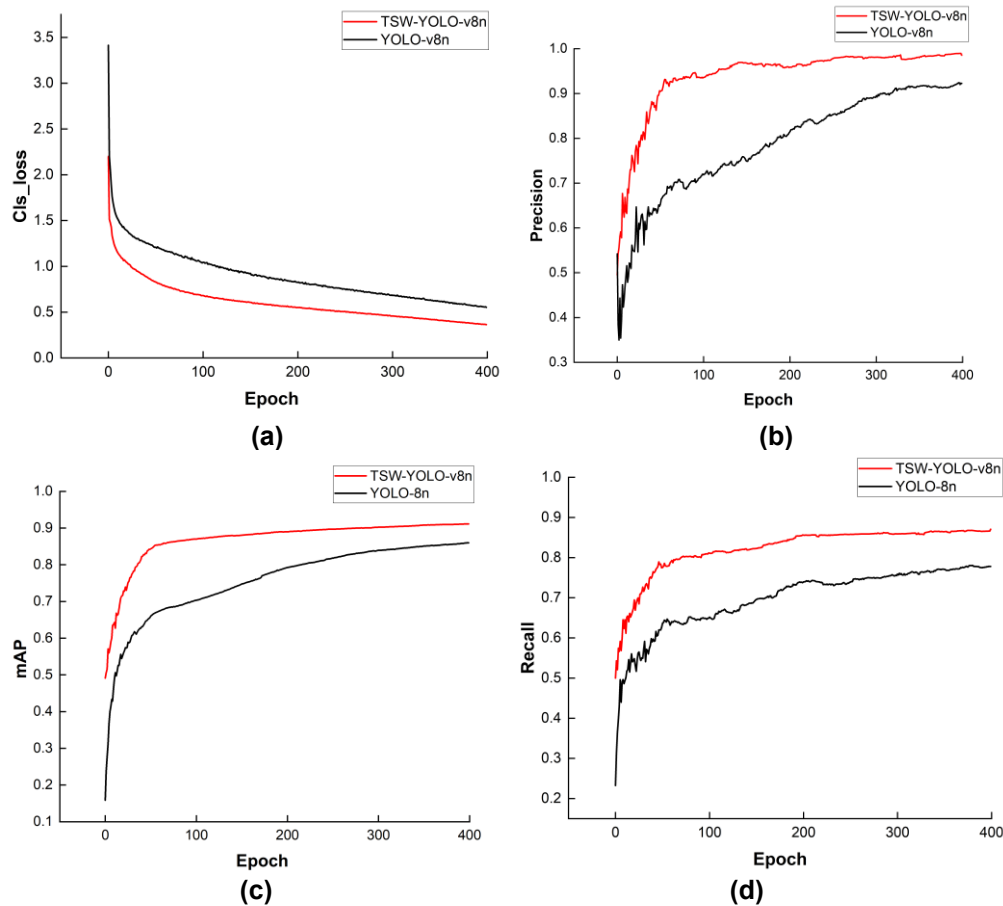


Fig. 6. Comparison between YOLO-v8n and TSW-YOLO-v8n

From the figure, it is evident that the improved TSW-YOLO-v8n model surpassed the original YOLO-v8n model across all metrics. Moreover, the trend of the curves reveals that the enhanced model maintained greater stability and exhibited superior detection performance throughout the training process.

Visual Results Analysis

In light of the challenge posed by the limited interpretability of deep learning models, an analysis was conducted of the model's detection performance improvement through two distinct lenses: the examination of the confusion matrix and a thorough evaluation of the model's inference results.

Confusion matrix result analysis

As evident from Fig. 7-a, the diagonal region of the confusion matrix in the enhanced TSW-YOLO-v8n model exhibited a notably darker hue compared to the diagonal region of the confusion matrix in YOLO-v8n, as depicted in Fig. 7-b. This discrepancy serves as a visual indicator of the improved model's heightened capability in detecting various defect categories to a significant extent.

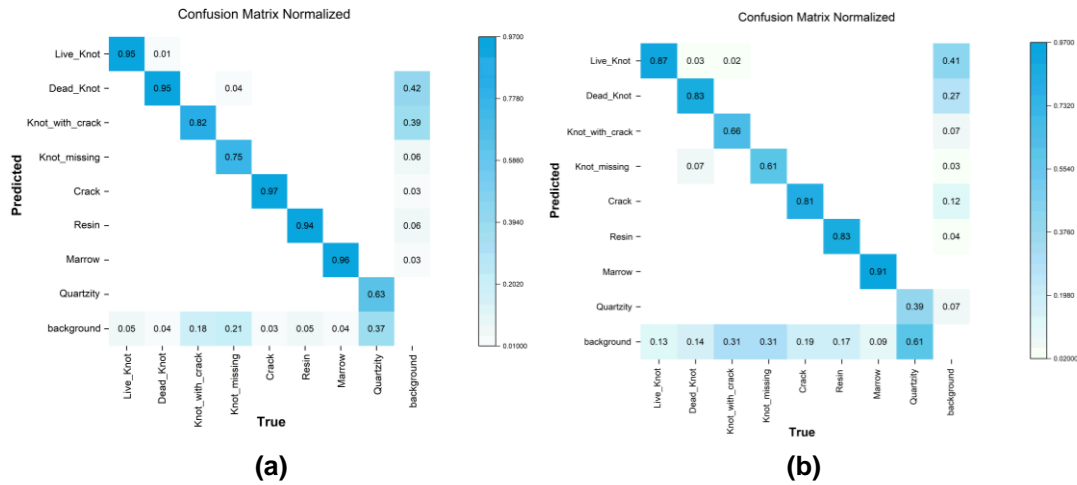


Fig. 7. (a) TSW-YOLO-v8n confusion matrix diagram; (b) YOLO-v8n confusion matrix diagram

Analysis of picture reasoning results

Eight sawn timber images were randomly selected to construct a graphical representation, and subsequently, defect detection was carried out using both the YOLO-v8n and the enhanced TSW-YOLO-v8n models. As depicted in Fig. 8-a, one live knot and one dead knot remained undetected, with a total processing time of 7 milliseconds. Conversely, the predictions generated by the improved TSW-YOLO-v8n model, illustrated in Figure 8-b, not only successfully identified the previously overlooked defects in Fig. 8-a but also accomplished this task within a reduced total processing time of 6 milliseconds.

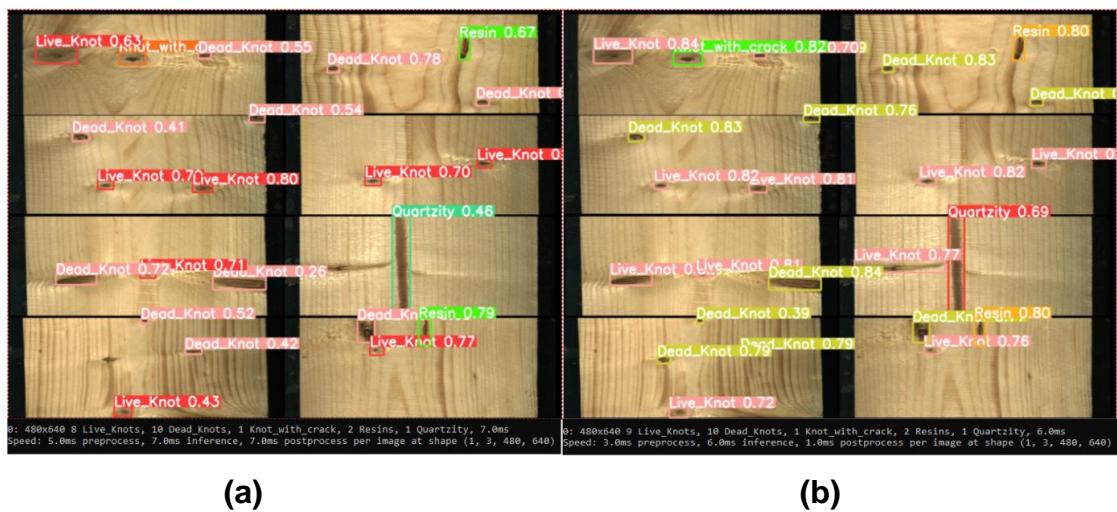


Fig. 8. (a) YOLO-v8n picture inference results ; (b) TSW-YOLO-v8n image inference results

While this paper’s improved method primarily targets the detection of small targets, it acknowledges that the enhancement in Quartzity is relatively modest, and the recognition accuracy remains suboptimal. Consequently, future research endeavors should concentrate on further optimizing the model’s detection accuracy, particularly in the context of small target defects.

CONCLUSIONS

1. In response to the prevalence of small defects such as live knots, dead knots, and cracks on the surface of sawn timber, coupled with the substantial fusion between sawn timber texture features and defects, this paper introduces a lightweight sawn timber surface defects detection model known as TSW-YOLO-v8n, which was built upon the YOLO-v8n framework.
2. The primary focus of the TSW-YOLO-v8n model lies in addressing the challenges posed by the detection of small, hard-to-identify defects and the substantial blending of defects with the background. To achieve this, the model employs an improvement strategy that enhances its performance while minimizing its computational footprint. Notably, the improved model enhances detection efficiency and accuracy, achieving a 5.1% increase in average detection accuracy compared to the original model. It accomplishes defect detection with an impressive elapsed time of 6 ms, significantly elevating its defect detection capabilities. Furthermore, the improved model surpasses mainstream algorithms in terms of detection accuracy.

ACKNOWLEDGMENTS

The authors are grateful for the support of the key R&D and achievement transformation plan of Inner Mongolia Autonomous Region, Project NO. 2022YFDZ0031.

REFERENCES CITED

- Cao, Y., Liu, F., Jiang, L., Bao, C., Miao, Y., Chen, Y. (2023). "Lightweight wood panel defect detection method incorporating attention mechanism and feature fusion network," *arXiv preprint arXiv:2306.12113*. DOI: 10.48550/arXiv.2306.12113
- Cui, Y., Lu, S., and Liu, S. (2023). "Real-time detection of wood defects based on SPP-improved YOLO algorithm," *Multimedia Tools and Applications*, 1-14. DOI: 10.1007/s11042-023-14588-7
- Fang, Y., Guo, X., Chen, K., Zhou, Z., Ye, Q. (2021). "Accurate and automated detection of surface knots on sawn timbers using YOLO-V5 model," *BioResources* 16(3), 5390-5406. DOI:10.15376/biores.16.3.5390-5406
- Han, S., Jiang, X., and Wu, Z. (2023). "An improved YOLOv5 algorithm for wood defect detection based on attention," *IEEE Access*. DOI: 10.1109/ACCESS.2023.3293864
- Kodytek, P., Bodzas, A., and Bilik, P. (2022). "A large-scale image dataset of wood surface defects for automated vision-based quality control processes," *F1000Research* 10, 581. DOI: 10.12688/f1000research.52903.2
- Kurdthongmee, W. (2023). "Improving wood defect detection accuracy with Yolo V3 by incorporating out-of-defect area annotations," *Preprint available at SSRN 4395580*. DOI: 10.2139/ssrn.4395580
- Liu, W., Anguelov, D., Erhan, D., Szegedy, C., Reed, S., Fu, C. Y., and Berg, A. C. (2016). "Ssd: Single shot multibox detector," in: *Computer Vision–ECCV 2016: 14th European Conference, Amsterdam, The Netherlands, October 11–14, 2016, Proceedings, Part I 14* (pp. 21-37). Springer International Publishing. DOI: 10.1007/978-3-319-46448-0_2

- Misra, D., Nalamada, T., Arasanipalai, A. U., and Hou, Q. (2020). "Rotate to attend: Convolutional triplet attention module," in: *Proceedings of the IEEE/CVF Winter Conference on Applications of Computer Vision*, pp. 3139-3148.
- Shih, K. H., Chiu, C. T., Lin, J. A., and Bu, Y. Y. (2019). "Real-time object detection with reduced region proposal network via multi-feature concatenation," *IEEE Transactions on Neural Networks and Learning Systems* 31(6), 2164-2173.
- Tan, M., Pang, R., and Le, Q. V. (2020). "Efficientdet: Scalable and efficient object detection," In *Proceedings of the IEEE/CVF Conference on Computer Vision and Pattern Recognition*, pp. 10781-10790.
- Tong, Z., Chen, Y., Xu, Z., and Yu, R. (2023). "Wise-IoU: Bounding box regression loss with dynamic focusing mechanism," *arXiv preprint arXiv:2301.10051*. DOI: 10.48550/arXiv.2301.10051
- Wang, B., Yang, C., Ding, Y., and Qin, G. (2021a). "Detection of wood surface defects based on improved YOLOv3 algorithm," *BioResources* 16(4), 6766-6780. DOI: 10.15376/biores.16.4.6766-6780
- Wang, Y., Zhang W., Gao R., and Jin Z. (2021b). "Identification of surface defects in structural sawn timber based on YOLOv4," *Journal of Forest Engineering* 6(4), 120-126. DOI:10.13360/j.issn.2096-1359.202010009
- Woo, S., Park, J., Lee, J. Y., and Kweon, I. S. (2018). "Cbam: Convolutional block attention module," in: *Proceedings of the European Conference on Computer Vision (ECCV)*, pp. 3-19.
- Yang, F., Wang, Y., Wang, S., and Cheng, Y. (2018). "Wood veneer defect detection system based on machine vision," in: *2018 International Symposium on Communication Engineering & Computer Science (CECS 2018)*, Atlantis Press, pp. 413-418.
- Zhu, H., Zhou S., Liu X., Zeng Y., and Li, S. (2023). "A review of single-stage object detection algorithms based on deep learning," *Industrial Control Computer* 36(04), 101-103.

Article submitted: September 11, 2023; Peer review completed: October 7, 2023; Revised version received and accepted: October 8, 2023; Published: October 26, 2023.

DOI: 10.15376/biores.18.4.8444-8457